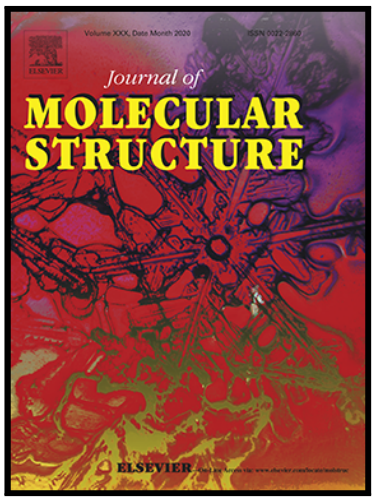

Cocrystallisation of Daidzein with Pyridine-derived Molecules: Screening, Structure Determination and Characterisation

Linzie Bolus , Ke Wang , Christopher Pask , Xiaojun Lai , Mingzhong Li

PII: S0022-2860(20)31218-7
DOI: https://doi.org/10.1016/j.molstruc.2020.128893
Reference: MOLSTR 128893

To appear in: *Journal of Molecular Structure*

Received date: 11 May 2020
Revised date: 29 June 2020
Accepted date: 13 July 2020

Please cite this article as: Linzie Bolus , Ke Wang , Christopher Pask , Xiaojun Lai , Mingzhong Li , Cocrystallisation of Daidzein with Pyridine-derived Molecules: Screening, Structure Determination and Characterisation, *Journal of Molecular Structure* (2020), doi: https://doi.org/10.1016/j.molstruc.2020.128893

Highlights

- Computational and experimental cocrystal screening of Daidzein against six coformers.
- A novel Daidzein-4,4'-Bipyridine cocrystal has been discovered and characterised.
- Cocrystal of Daidzein-4,4'-Bipyridine is connected through intermolecular hydrogen bond interactions.
- The cocrystal of Daidzein-4,4'-Bipyridine shows increased solubility and dissolution rate compared to Daidzein.

Cocrystallisation of Daidzein with Pyridine-derived Molecules: Screening, Structure Determination and Characterisation

Linzie Bolus[1], Ke Wang[1], Christopher Pask[2], Xiaojun Lai[2], Mingzhong Li[1*]

[1]School of Pharmacy, De Montfort University, Leicester, LE1 9BH, UK

[2]Faculty of Engineering and Physical Sciences, University of Leeds, Leeds, LS2 9JT, UK

Graphic Abstract

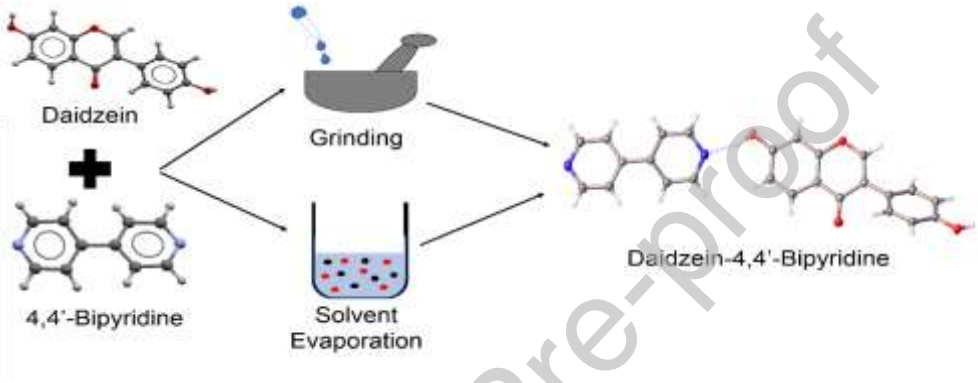

Abstract

Daidzein (7,4'-dihydroxyisoflavone, DAI) is an isoflavone found in soybeans and Pueraria. DAI has potential therapeutic benefits on cancer and osteoporosis yet has quite low solubility, limiting its use. Herein a cocrystal screening of DAI with pyridine-derived molecules, i.e., nicotinamide, isonicotinamide, caffeine, D-Proline, L-Proline and 4,4'-Bipyridine was conducted. A new cocrystal of Daidzein and 4,4'-Bipyridine (DAI-BIP) was successfully generated via grinding and solvent methods. DAI-BIP showed an increased solubility and dissolution rate. In comparison to DAI, there was a 2.03-fold increase of the dissolution performance parameter for DAI-BIP where the concentration observed for DAI quickly reached the equilibrium solubility and continued to reach 1.49 times DAI solubility. A parachute effect was also observed during the dissolution of DAI-BIP, indicating that BIP might be able to maintain the supersaturated state of DAI in solution proving DAI's ability to form cocrystals of higher solubility and enhanced dissolution properties through co-crystallisation.

*Corresponding Author: Email:mli@dmu.ac.uk; Tel: +44(0)116 257 7132.

Key words: Cocrystal; Daidzein; 4,4'-Bipyridine; Screening; Solubility; Dissolution rate.

1. Introduction

Flavonoids are a group of polyphenols, which have a 15-carbon skeleton, consisting of two aromatic rings connected by a 3 carbon bridges shown in Fig. 1(a). They are common classes of nutraceuticals which can be found in fruits, vegetables, cereals, legumes, chocolate, and beverages (i.e., tea, coffee or wine) [1, 2]. Flavonoids have shown numerous health and medical benefits, including antioxidant, hypocholesterolemic, anti-inflammatory effects as well as the ability to modulate cell signalling and gene expression related disease development [3, 4]. Despite their well-recognised health and medical benefits, flavonoids hold intrinsic physiochemical disadvantages, e.g. poor solubility, permeability and inferior stability, resulting in extremely low bioavailability of the oral dosage form [2, 3]. In order to increase the bioavailability of flavonoids, various strategies have been developed, including absorption enhancers, structural transformation (e.g., prodrugs, glycosylation), novel delivery systems (e.g., carries, complexes, nanotechnology, cocrystals), and changing the site of absorption (e.g., from large intestine to small intestine) [5, 6].

In recent years, pharmaceutical cocrystals have drawn a significant amount of interest for their ability to modify physicochemical properties of active pharmaceutical ingredients (APIs), in particular enhancing solubility and dissolution rate of poorly water-soluble drugs, through supramolecular interactions between an API and coformer [7]. Intense effort has been made to design oral form nutraceutical cocrystals which have maximized bioavailability and efficacy [8-14]. Selection of an appropriate coformer for a given API is key for success in cocrystal design as the coformer can have a huge impact on the cocrystals resulting properties. Intermolecular interaction complementarity and supramolecular synthon hierarchy are most commonly used as an empirical guideline for the coformer selection of cocrystal design [15-17], although many computational tools have been applied for cocrystal screening [18-21]. It has been found that pyridine-derived molecules, such as nicotinamide, isonicotinamide, and 4,4'bipyridine, were the highly regarded coformers to cocrystallise with a flavonoid, presenting an O-H···N_{arom} heterosynthon between an O7 hydroxyl moiety of a flavonoid and the pyridyl ring of a coformer [8-14, 22-27]

Daidzein [7,4'-dihydroxyisoflavone, DAI shown in Fig. 1(b)] is a natural isoflavone compound that is abundant in soybean and Pueraria [28]. DAI is of pharmaceutical interest due to its potential therapeutic effects against cancer, osteoporosis and inflammation [29, 30]. However, the poor solubility (3.01 μg/mL at 35°C in water) of DAI [31] resulted in low oral bioavailability (6.1%) and very limited clinical application [32]. So far, there is no DAI cocrystal in the CSD (Cambridge Structural Database) reported. Although several daidzein cocrystals were reported, there was no single cocrystal successfully grown for its structure determination [33, 34]. Therefore, discovery of new cocrystal forms of DAI with their structure determined is extremely important for potential development of oral dosage form with improved physicochemical properties.

In this work, pre-screening was undertaken using both the CSD multi-component screening and molecular electrostatic surface potential tools to determine the probability of cocrystal formation of

DAI with the pyridine-derived coformers, i.e., nicotinamide, isonicotinamide, L-Proline, D-Proline and Caffeine, and 4,4'-bipyridine (Fig. 1c-1h). Experimental screening was conducted by co-grinding a 1:1 stoichiometric ratio mixture of DAI and a coformer with or without different solvents for 30 min. The samples were analysed by PXRD (power x-ray diffraction), FTIR (Fourier transform infrared spectroscopy), and thermal analysis (DSC and hot stage microscopy) for confirmation of cocrystal formations. It was found that only 4,4'-Bipyridine can form cocrystals with daidzein (DAI-BIP). Solution evaporation experiments of DAI and BIP were subsequently undertaken to obtain single cocrystals suitable for structure determination using single XRD analysis. The pharmaceutical relevant properties of solubility curve and dissolution rates of the cocrystals have been evaluated.

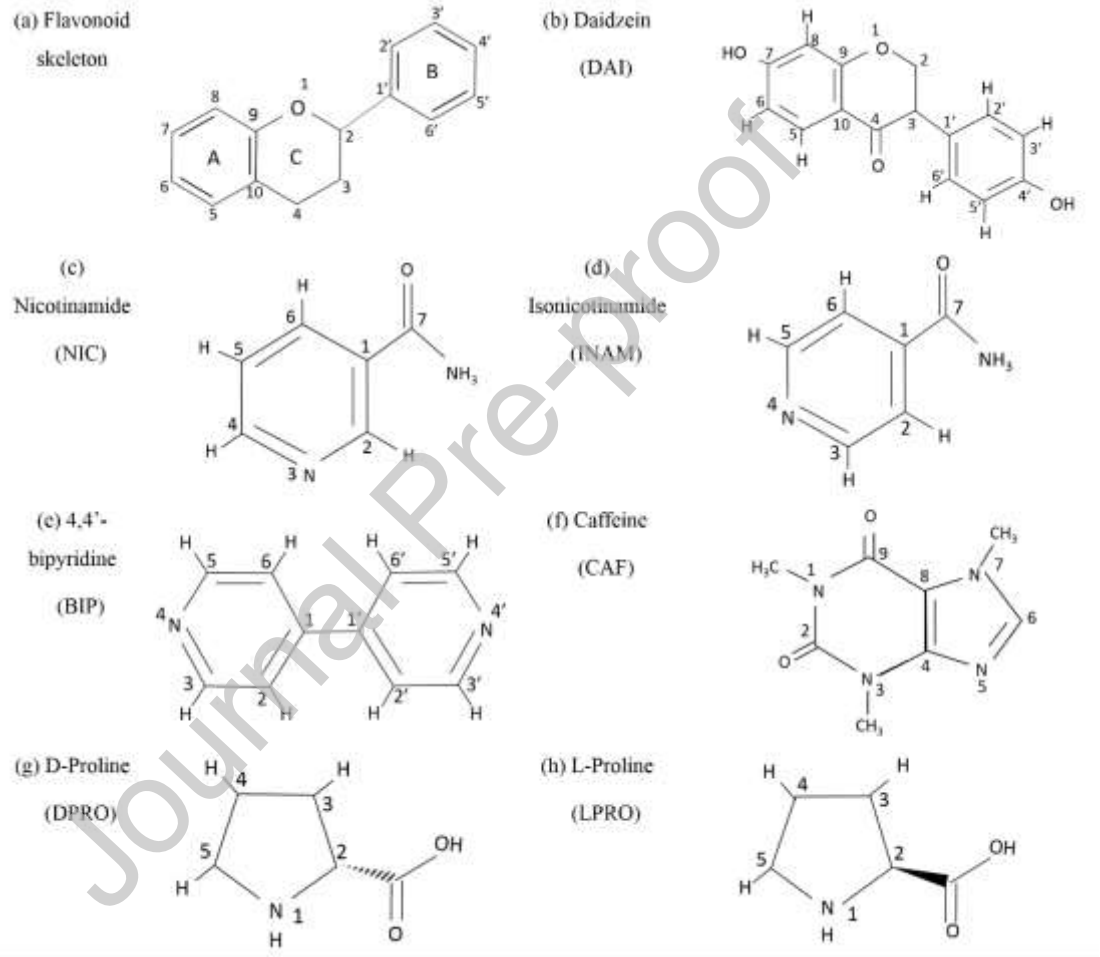

Fig. 1: Chemical structures of flavonoid skeleton (a), Daidzein (b), Nicotinamide (c), Isonicotinamide (d), 4,4'-bipyridine (e), Caffeine (f), D-Proline (g) and L-Proline (h)

2. Materials and methods

2.1 Materials

Daidzein (DAI) (≥97% purity), Isonicotinamide (INAM), L-Proline (LPRO) and D-Proline (DPRO) (all with ≥99% purity) was purchased from Alfa Aesar (Lancaster, UK). Caffeine (CAF), 4,4'-Bipyridine (BIP) (≥99% purity), Methanol (MeOH) (HPLC grade), Ethanol (EtOH) (HPLC

grade), Acetonitrile (ACN) (HPLC grade), Formic Acid 0.25M (HPLC grade), Tetrahydrofuran (THF) (extra dry), Chloroform (CF), Acetone (ACE) (reagent grade) and Ethyl Acetate (EtAC) (reagent grade) were purchased from Fisher Scientific UK (Loughborough, UK). Nicotinamide (NIC) (≥99.5% purity) was purchased from Sigma-Aldrich (Dorset, U.K). Double distilled water (DDW) was generated using a Bi-Distiller (WSC044.MH3.7, Fistreem International Limited, Loughborough, U.K.) in house and used for the duration of the study.

2.2 Methods

2.2.1 0.01 M pH 6.8 Phosphate Buffer solution (PBS) preparation

pH 6.8 PSB solution (0.01 M) was used as media for solubility and dissolution studies. It was prepared according to British Pharmacopeia 2010, i.e., 1.365g of potassium dihydrogen phosphate (KH_2PO_4) was dissolved in DDW and the pH of the solution was adjusted to 6.8 by 1 M sodium hydroxide addition.

2.2.2 Ab initio screening

An initial cocrystal screening was undertaken by the CSD search (ConQuest v2.0.1) using the key words of Daidzein and its molecular structure. Cocrystals of nutraceuticals with similar structures as DAI were also searched for selection of potential coformers used in experiments for DAI cocrystal screening. The pass or fail of formation of cocrystals of between DAI and a chosen coformer was evaluated by the CSD multi-component screening tool (Mercury v4.1.0).

Furthermore, the probabilities of cocrystal formations of between DAI and coformers were calculated using the virtual cocrystal screening tools [18], in which an energy difference was calculated based on gas phase molecular electrostatic potential surfaces (MEPSs) of the individual compounds (Spartan18, v1.3.0).

2.2.3 Cocrystal screening via neat grinding (NG) and liquid-assisted grinding (LAG)

In the screening experiments, a total of 200 mg of DAI and either BIP, NIC, LPRO, DPRO, CAF or INAM at a 1:1 stoichiometric ratio was prepared in 15 mL stainless steel SmartSnap™ jars containing two 7mm stainless steel grinding balls (Form-Tech Scientific, Montreal, Canada). For a LAG experiment, 40 µL of solvent (ACE, ACN, CF, DDW, EtAC, EtOH, MeOH or THF) was added. Materials were ground in a Retsch Mixer Mill MM 400 (Retsch, germany) for 30 min at a rate of 25 Hz at room temperature. DAI with INAM was also subjected to grinding in a 1:2 stoichiometric ratio. Samples were left to stabilise for 30 min before characterisation by PXRD and thermal methods.

2.2.4 Preparation of cocrystal powders and single cocrystal

Daidzein-4,4'-bipyridine cocrystals (DAI-BIP) in a 1:1 stoichiometric ratio were prepared by solvent evaporation (SE). A 1:1 equimolar mixture of DAI and BIP was dissolved in a solvent mixture of EtAC and EtOH (87%:13%). Solution was stirred at 50°C until all solids dissolved before being left in a fume cabinet for evaporation. The formation of cocrystals was confirmed by PXRD, FTIR, DSC and hot stage microscopy (HSM).

Single cocrystals were also prepared using this method, but the solution was slowly evaporated over a period of one month and harvested by natural filtration. Crystals were characterised by single XRD, FTIR and HSM.

2.2.5 Solubility studies

Apparent equilibrium solubility of DAI was measured by adding excess amount of crystalline materials to a small vial containing 20 mL of pH 6.8 PBS, which was kept at 37 ± 0.5°C in a shaking water bath at 150 rpm for 24 h. The supernatant was separated from the suspension by a micro centaur MSB 010.CX2.5 centrifuge (MSE Ltd., London, U.K.) at 13000 rpm for 1 min. The supernatant was then diluted to determine the concentration of DAI by HPLC. The cocrystal solubility was determined by measuring the eutectic point of the cocrystals [35]. A series of BIP solutions were prepared in pH6.8 PBS at concentrations of 0, 2, 3.8, 4.2, 4.4, 4.6, 4.8, 5, 5.2, 6, 8 mg/mL. Excess amount of DAI as added to a small vial with 20 mL of each of the prepared BIP solutions, which were kept in a shaking water bath at 37°C ± 0.5°C and a shaking rate of 150 rpm for 24 h. The supernatant of each suspension was separated by centrifuge whilst all solid residues were separated by filtration. The concentrations of DAI and BIP in the supernatant were analysed by HPLC and UV respectively. The solid residues were dried naturally and then analysed by PXRD. The eutectic point of the cocrystals was determined by the lowest BIP concentration solution where two solid phases of DAI and cocrystal coexisted in equilibrium with the solution.

All experiments above were repeated in triplicate.

2.2.6 Powder Dissolution studies

Powder dissolution experiments of DAI and DAI-BIP were performed under non-sink conditions in pH6.8 PBS. All materials were ground using a mortar and pestle and sieved by a 60 mesh sieve (below 250 µm) to reduce the effect of particle size on the dissolution rates. Each of dissolution tests was carried out via USP Apparatus 2 (paddle) at a speed of 50 rpm in 400 mL of dissolution medium maintained at 37±0.5 °C using a PTWS 120D dissolution bath fitted with a variable speed stirrer and heater (Pharma Test). The cocrystals used in the dissolution tests had the equivalent amount of the parent nutraceutical, i.e., 21 mg of DAI-BIP and 13 mg of DAI. Samples of 1±0.1 mL were removed at the predefined time points of 5, 15, 50, 60, 120, 180 and 240 min. Supernatants were separated from the samples and analysed by HPLC and UV to determine DAI and BIP concentrations respectively. All experiments were repeated in triplicate.

2.2.7 Cocrystal Characterisation

1) Powder X-ray diffraction analysis (PXRD) and prediction

Samples were analysed by a Bruker D2 phaser diffractometer equipped with a LYNXEYE XE-T detector (Bruker UK Limited, Coventry, UK). The diffractometer was operated at 10mA and 30 kV. All samples were analysed under room temperature in the 2θ range of 2-40° at a scanning rate of 0.4° (2θ) min^{-1}.

A simulated PXRD pattern of DAI-BIP from the single crystal structure was performed using the powder pattern tool in Mercury v4.20 (Cambridge Crystallographic Data Centre). Analysis range of degrees 2θ was set from 5-40° with a scanning step size of 0.02° (2θ) at a wavelength of 1.54056 Å. The pattern was set to include hydrogens.

2) Single X-ray diffraction analysis (SXRD)

Measurements were carried out at 125K on an Agilent SuperNova diffractometer equipped with an Atlas CCD detector and connected to an Oxford Cryostream low temperature device using mirror monochromated Cu Kα radiation (α = 1.54184 Å) from a Microfocus X-ray source. The structure was solved by intrinsic phasing using SHELXT1 and refined by a full matrix least squares technique based on F2 using SHELXL2014[36, 37].

All non-hydrogen atoms were located in the Fourier Map and refined anisotropically. All carbon-bound hydrogen atoms were placed in calculated positions and refined isotropically using a "riding model". Oxygen-bound hydrogen atoms were located in the Fourier Map and refined isotropically.

3) Fourier-Transform Infrared spectroscopy (FTIR)

FTIR spectra were collected on an ALPHA interferometer (Bruker UK Limited, Coventry, UK) equipped with a horizontal universal attenuated total reflectance (ATR) accessory. Data was collected for each sample, between 400-4000 cm^{-1} using 30 scans at a resolution of 2 cm^{-1} by the OPUS software at room temperature.

4) Differential scanning calorimetry (DSC)

The cocrystal melting point was determined using a PerkinElmer Jade DSC (PerkinElmer Ltd., Beaconsfield, UK) operated under a nitrogen atmosphere. The instrument was calibrated using indium metal. A heating rate of 20°C/min in a range of 80-360°C was employed for samples (sample mass approximately 8mg) in aluminium pans with pinhole lids.

5) Hot stage microscopy (HSM)

A Mettler Toledo FP82HT hot stage and FP90 controller (Mettler Toledo, Ohio, United States) was used to monitor the thermal events of the cocrystals during heating. The hot stage was connected to a Leica DM750 microscope (Leica Microsystems (UK) Ltd, Milton Keynes, UK). Sample was prepared on a slide to cover the pinhole of the hot stage. A heating rate of 20°C/min in a range of 80-360°C was employed for samples. The video of melting was captured on StudioCapture software.

6) High-performance liquid chromatography (HPLC)

Concentrations of DAI in solution were analysed using a PerkinElmer series 200 HPLC (PerkinElmer Ltd. Beaconsfield, UK) with a HAISLL 100 C18 column (5 µm, 250 ×4.6 mm) (Higgins Analytical Inc., Mountain View, CA, USA) at 30°C. An isocratic method with 50% double distilled water (including 1% formic acid) and 50% acetonitrile at 0.5 mL/min flow rate and a detection wavelength of 248 nm were used to detect DAI concentration.

7) UV spectroscopy (UV) to detect BIP concentration

Concentrations of BIP in solution were analysed using a Thermo Scientific Evolution 60s UV spectrophotometer (Fisher Scientific UK Ltd. Loughborough, UK) at room temperature. The UV spectrometer was blanked using phosphate buffer and samples were analysed at 235 nm.

3. Results and discussion

3.1 Ab initio screening

Twenty-five structures were retrieved based on the CSD search using the key words of Daidzein and its molecular structures detailed in Table S1 in the supplementary information. There are four polymorphs of DAI, with space groups of $P2_1/c$, $P\bar{1}$, $P2_1/n$ and $P2_12_12_1$ [28]. Nine structures correspond with solvates or derivatives of DAI. There are no DAI cocrystals deposited. Interestingly the other 13 hits are related to Genistein (GEN), another natural isoflavone compound having similar molecular structure as DAI [13]. Among them, six GEN cocrystals are found, i.e., Genistein-4,4'-Biprydine (GEN-BIP), Genistein-L-Proline (GEN-LPRO), Genistein-D-Proline (GEN-DPRO), Genistein-Isonicotinamide (GEN-INAM), Genistein-Nicotinamide (GEN-NIC) and Genistein-Caffeine (GEN-CAF). Therefore, these coformers were selected for screening of DAI cocrystals.

Based on a pass or fail prediction by the CSD multi-component screening tools, it was found that BIP, INAM and NIC can form cocrystals with DAI whereas LPRO/DPRO and CAF failed the initial screening (Table S2 in the supplementary information). Furthermore, the probability of cocrystal formation between DAI and a coformer selected was calculated using the virtual cocrystal screening tools [18]. After geometry optimisation, the MEPSs of DAI and six coformers were generated using Spartan18 (v1.3.0) shown in Fig. 2. Potential hydrogen bonding sites of DAI with coformers are the two maximal positive potential regions at hydrogens of the hydroxyl groups located at C7 and C4' and two minimal negative potential regions at oxygens located at C1 and C4 on DAI's MEPS [Fig. 2(a)]. The difference between the interaction site pairing energies of the potential 1:1 cocrystal and two pure compounds and its probability of a cocrystal formation are shown in Table 1. It is shown that BIP has the highest probability to form a cocrystals with DAI at 16.70% and Isonicotinamide has the lowest probability at 2.48%. However, none of the probabilities is higher than 50%, even with variable stoichiometric ratios (the probabilities of formations of 1:2 cocrystals shown in Table. S3 in the supplementary information), indicating that all coformers selected are unlikely to form cocrystals with DAI. This is contradictive to the predictive results based on the CSD multi-component screening tools.

Compound	Molecular Electrostatic Potential Map
DAI (a)	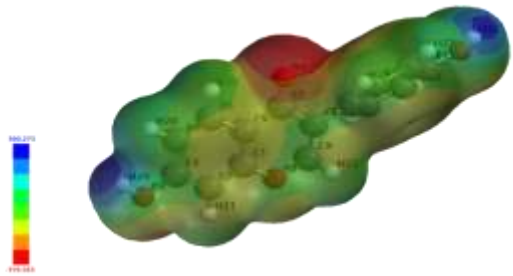
BIP (b)	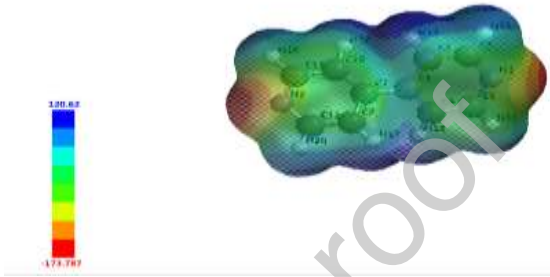
INAM (d)	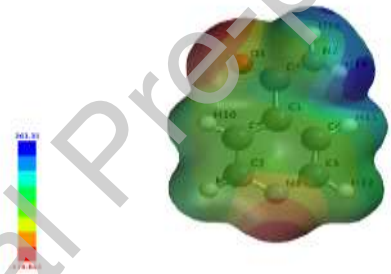
NIC (d)	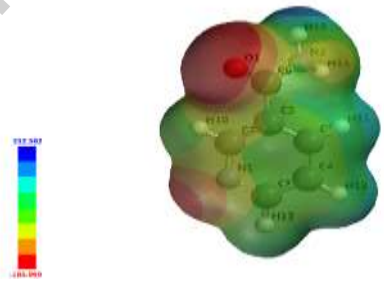
LPRO (e)	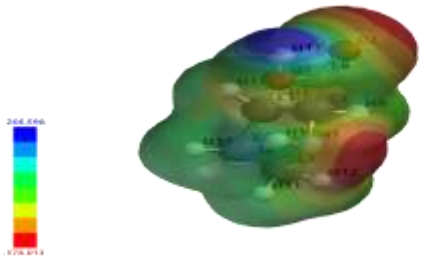

DPRO

(f)

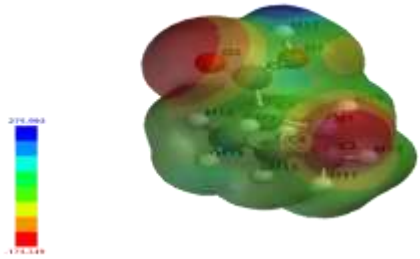

CAF

(g)

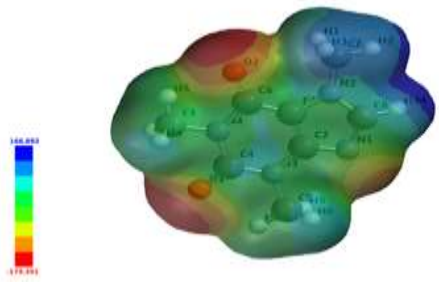

Fig. 2: Molecular Electrostatic Potential Surfaces

Table 1. Interaction site pairing energy difference and probability of cocrystal formation in a 1:1 stoichiometric ratio with daidzein

Coformer	Ratio	Interaction site pairing energy difference (ΔE), kJ/mol	Probability of formation (%)
BIP	1:1	-7.02	16.70
INAM	1:1	-1.90	2.48
NIC	1:1	-2.56	3.21
LPRO	1:1	-4.37	6.44
DPRO	1:1	-4.19	6.02
CAF	1:1	-6.58	14.42

3.2 Experimental screening

After computational screening, experimental screening via grinding was conducted. The grinding results for DAI-CAF, DAI-DPRO, DAI-LPRO and DAI-NIC were all negative as there was no new peak appeared or loss of characteristic peaks of the starting materials of DAI and coformer [Fig. S1 (i)-(iv) in the supplementary information]. The XRD patterns of ground DAI and INAM mixtures in 1:1 and 1:2 initially exhibited changes which were thought to be the formation of cocrystals of DAI-INAM (Fig. S2 in the supplementary information). Yet upon further investigation, it was found to be the effect of grinding INAM (Fig. S3 in the supplementary information), no DAI-INAM cocrystal had been formed which was consistent with expectation of the low probability of formation (2.48%) in computational screening. Screening experiments of 1:1 molar mixture of DAI and BIP showed that new crystalline phases of DAI-BIP can be formed by LAG in the presence of 40 µL of solvent of

EtAC shown in Fig. 3, where key characteristic peaks of DAI disappeared at 6.08°, 8.36°, 15.78° and 18.86° of 2θ and new peaks appeared at 11.51°, 12.67°, 15.04° and 18.24° of 2θ. The mixture of DAI and BIP by LAG in the presence of 40 µL of either ACE, ACN, CF, MeOH or THF also led to DAI-BIP cocrystal formation confirmed by PXRD patterns in Fig. S4 in the supplementary information. There was no cocrystal formation by LAG in the presence of a drop of EtOH and only partial transformation was seen in NG shown in Fig. S4 in the supplementary information. Phases of BIP can be affected by LAG in the presence of a drop of DDW shown in Fig. S5 in the supplementary information, causing the appearance of "new" peaks. The new peaks of the mixture of DAI and BIP by LAG in the presence of a drop of DDW belong to the change of BIP new peaks and partial transformation to the cocrystals shown in Fig. S4.

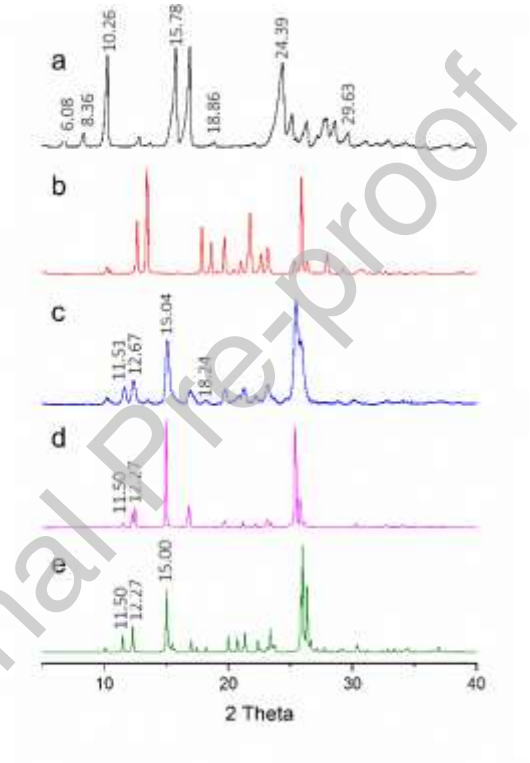

Fig. 3: PXRD patterns of DAI (a), BIP (b), DAI-BIP by LAG in the presence of EtAC (c), DAI-BIP from solvent evaporation (d), and DAI-BIP XRD simulation (e)

The XRD pattern of DAI-BIP powders from solvent evaporation is shown in Fig. 3(d), which is consistent with that of DAI-BIP by LAG in the presence of EtAC. Cocrystal powders of DAI-BIP were prepared by solvent evaporation using a mixture of EtAC (87%) and EtOH (13%) to ensure to fully dissolve the components in solution because of the very poor solubility of DAI in EtAC alone. The percentage of EtOH in the mixture played a key role for formation of DAI-BIP. It was found that the pure cocrystals of DAI-BIP cannot be formed if the percentage of EtOH in the mixture was higher than 13%. Effect of the ratio of EtAC and EtOH in the solvent mixture on the formation of DAI-BIP was given Fig. S6 in the supplementary information.

The thermal behaviours of the DAI-BIP powders synthesised were investigated using HSM shown in Fig. 4. A cocrystals melting point is usually found to be in between the starting materials melting points. DAI displayed a melting activity at 335.3°C and BIP melted at 115.7°C. The high melting point of DAI caused BIP to vaporise at a temperature of 197.3°C, HSM allowed visible confirmation of the vaporisation. The DAI-BIP showed an endothermic peak at 234°C, which corresponded to its melting point in between the original melting points of both DAI and BIP. After the DAI-BIP melting at 234°C, two endothermic peaks at 336°C and 344°C were found, corresponding to DAI melting point and, potentially, vaporisation of DAI (Fig. 4). The difference in the melting point of DAI-BIP is likely due to the change of packing of raw DAI compared to DAI in DAI-BIP. It is true that in most cases, cocrystals have different melting points in comparison to the individual components, which has been demonstrated to be dependent on their packing and stoichiometric ratio [17]. The herringbone packed systems displayed a melting point in between the two components as was the case in our study, while the crystal with a channel packing exhibited a melting point much lower than both components. Similar results were observed by DSC measurements shown in Fig S7 in the supplementary information.

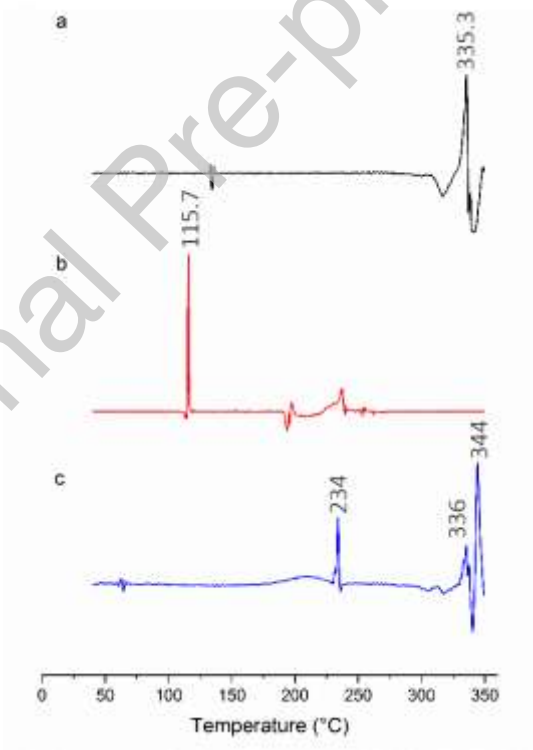

Fig. 4: HSM diagrams of DAI (a), BIP (b) and DAI-BIP via Solvent Evaporation (c)

3.3 Single cocrystal structure analysis

High quality single crystals of DAI-BIP for SXRD measurements were obtained through slow evaporation in a mixture of EtAC (87%) and EtOH (13%). DAI-BIP crystallises as orange coloured pinacoidal crystals like that of Rhodonite [Fig. 5(a) and Fig. S9 in the supplementary materials]. The

crystal structure of DAI-BIP was then determined by single XRD (SXRD) and FTIR analysis (Fig. S8 in the supplementary) was used to confirm cocrystal formation. DAI-BIP crystallises in the $P_{\overline{1}}$ space group of triclinic system with the cell parameters a = 7.9052 (4)Å, b = 10.4920(6) Å, c = 12.1115(7) Å and α = 102.434(5)°, β =101.212(5)°, γ =95.900(5)°. The cocrystal asymmetric unit is connected through intermolecular interactions between one molecule of DAI and one molecule of BIP (z=2).

Analysis of the packing in the cocrystal revealed that DAI and BIP were connected through O(1)—H···N(4') and O(2)—H···N(4) intermolecular interactions, forming a 1D hydrogen-bonding chain structure, which extended indefinitely along the *a* axis in the *ab* plane. The 1D chain structure extends via the b axis via C(2')—H ··· O(2) interactions between one BIP and one DAI molecule to form the 2D sheet structure (Fig. 5(c)). The distance between the two chains varied from 3.814 Å to 5.662 Å, suggesting that the π···π stacking interactions amongst the aromatic rings could be ignored. The 3D packing structure of the cocrystal (Fig. 5(d)) was formed by extending the 2D structure along the *ac* plane via multiple short contacts between either one DAI and one BIP molecule, or between two molecules of BIP. The morphology of the cocrystal was predicted, based on the crystallographic data, using the Bravais-Friedel-Donnay-Harker (BFDH) morphology tool from the Mercury software (Cambridge Crystallographic Data Centre Mercury v4.20) (Fig. 5(e)). The predicted morphology matched well with the experimental single crystal (Fig. 5(a)). Meanwhile, the simulated XRD pattern of the cocrystal was shown in Fig. 3(e). It illustrated all the characteristic peaks, which matched with what have been measured, including those at 11.50°, 12.27° and 15.00° of 2θ.

The SXRD measurements of the DAI-BIP single crystals have been deposited with the Cambridge Crystallographic Data Centre (CCDC) with the depositary number 1964859 and the crystallographic data is also shown in table S4.

a 

b 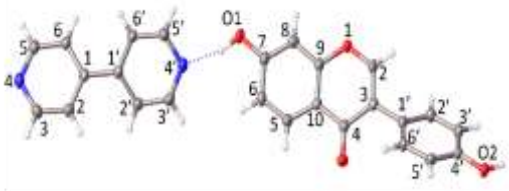

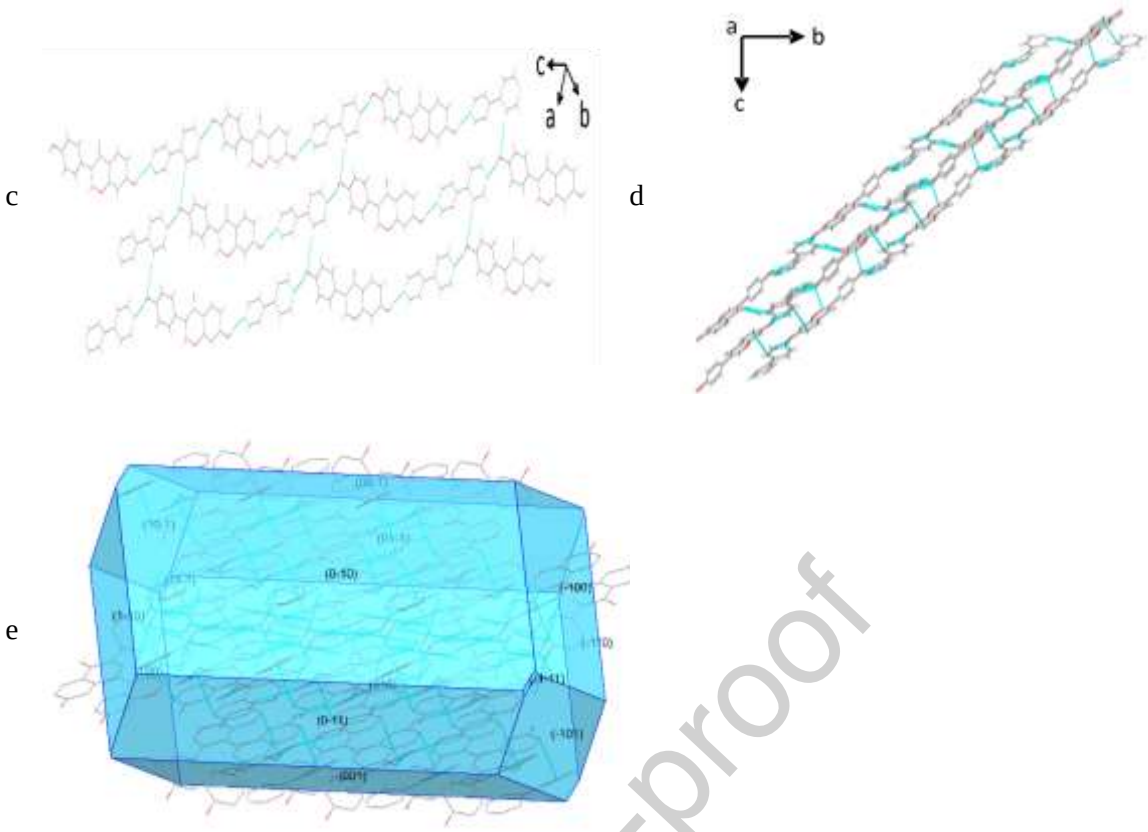

Fig. 5: The structure and packing of DAI-BIP. a) Single crystal under polarised light microscope; b) supramolecular synthon; c) 2D packing; d) 3D packing; e) Predicted morphology

3.4 Solubility and dissolution studies

The solubility and dissolution rate of the cocrystal and its components were examined. It was shown that the equilibrium solubility of DAI (i.e. dissolved drug concentration at equilibrium with solid drug) was 3.876±0.039 µg/mL (0.0152±1.52 0E-04 mM) in pH6.8 PBS at 37 °C, which is also pH-independent (Fig. S10).

The apparent concentration of DAI was measured in the presence of BIP (Fig. 6(a)) in pH6.8 PBS at 37 °C. The apparent concentration of DAI at equilibrium increased when the concentration of BIP increased to 3.8 mg/mL, indicating a formation of the DAI-BIP complexes. Within this range, the concentration of DAI-BIP hasn't exceeded its solubility limit, thus there was no precipitation of the cocrystal. Therefore, any solid residues observed within such range should be DAI alone, as confirmed by PXRD (Fig. 6(b)). When the concentration of BIP was higher than 3.8 mg/mL, the apparent concentration of DAI at equilibrium decreased. At a BIP concentration of 4.4 mg/mL, the precipitation of DAI-BIP started and two phases, DAI and DAI-BIP, could be observed for the solid residues in the solution [Fig. 6(b)]. The concentrations measured for DAI and BIP in the 4.4 mg/mL BIP solution represented the transition concentration of DAI-BIP [35], i.e. 0.045 mM for DAI and 28.171 mM for BIP. So, according to the definition of cocrystal solubility [35], the solubility of DAI-BIP was 1.122mM, which was 73.5-fold higher than the solubility of DAI. The higher DAI

concentration from the cocrystals at equilibrium can be attributed to the improved cocrystal dissolution rate and molecular interaction between DAI and BIP in solution. The hydrogen bonding between DAI and BIP allows the DAI to dissolve more easily whilst dissuading cocrystal disintegration back into starting materials by the molecular interaction via BIP in solution, therefore, increasing the solubility of the cocrystals. The higher concentration of DAI from the cocrystals at equilibrium was expected due to the decrease in melting point for the cocrystals compared to DAI [27] .

(a)

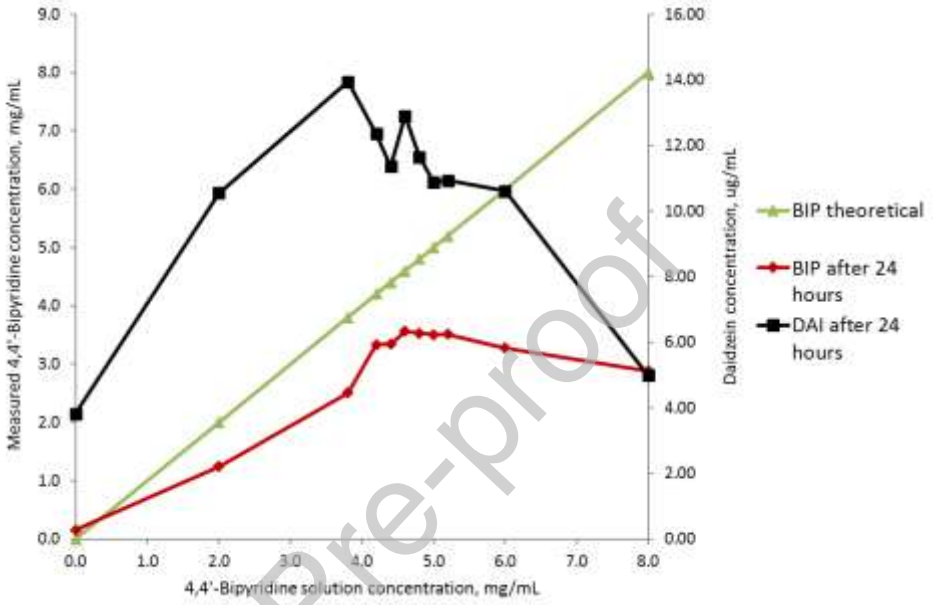

(b)

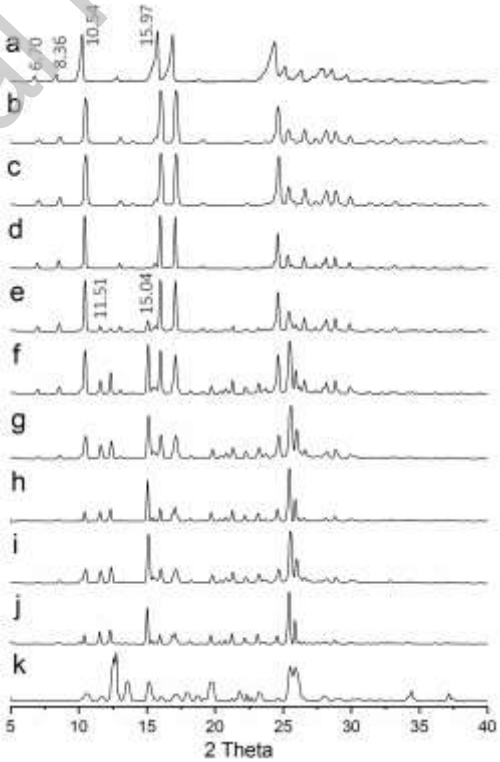

Note: a) 0 mg/mL b) 2 mg/mL, c) 3.8 mg/mL, d) 4.2 mg/mL, e) 4.4 mg/mL, f) 4.6 mg/mL, g) 4.8 mg/mL, h) 5 mg/mL, i) 5.2 g/mL, j) 6 mg/mL and k) 8

mg/mL

Fig. 6: Apparent solubility of DAI in the presence of BIP at different concentrations. (a) The concentrations of DAI and BIP at equilibrium; (b) PXRD observations of the solid residues

The dissolution profiles of DAI and DAI-BIP were illustrated in Fig. 7. The dissolution rate of DAI was significantly slower and, after 4 hours, its concentration was 2.830 ± 0.004 ug/mL. In contrast, the dissolution rate of DAI-BIP was greatly improved and, within 20 minutes, the concentration of DAI quickly reached its equilibrium solubility of 3.876±0.039 µg/mL. The concentration of DAI released from the cocrystal continued to increase until it reached 5.76 µg/mL, which was 1.49 times DAI solubility. During dissolution, a parachute effect was observed, indicating that the BIP might be able to maintain the supersaturated state of DAI in solution alone without the use of an additional precipitation inhibitor e.g. a polymer. In terms of the dissolution performance parameter (DPP) [35], DAI-BIP showed a 2.03-fold increase in comparison to DAI. This is due to BIP delivering DAI into the solution, aided by the heterosynthon, at a more rapid rate and causing a higher concentration at equilibrium whilst retarding the precipitation and recrystallisation of DAI out of solution. It was also worth noting that the solid residues, following dissolution of DAI-BIP, were DAI, as confirmed by PXRD (Fig S11), suggesting an occurrence of phase transformation during the dissolution of DAI-BIP.

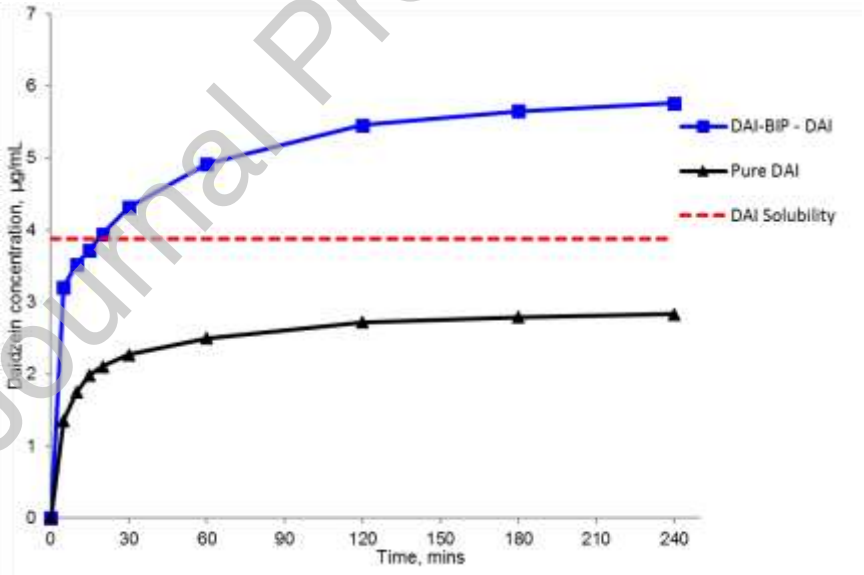

Fig. 7: Profiles of powder dissolution for DAI and DAI-BIP under non-sink conditions.

4. Conclusion

DAI has many potential therapeutic benefits which has attracted attention from scientists and industry. The limitation of DAI's solubility and bioavailability can be improved by solubility enhancement methods such as co-crystallisation. Pyridine-derived molecules (such as nicotinamide,

isonicotinamide and 4,4'-Bipyridine) offer an O-H···N_{arom} heterosynthon between the flavonoid and the pyridyl ring of the coformer. Computational screening provided an initial prediction for the successful preparation of novel nutraceutical cocrystal of Daidzein and 4,4'-Bipyridine (DAI-BIP) via grinding and solution methods. DAI-BIP belonged to the $P\bar{1}$ space group of the triclinic system formed N4'$_{arom}$···H—O—C7 and C4'—O4—H···N4$_{arom}$ intermolecular interactions between DAI and BIP. DAI-BIP showed increased solubility and dissolution performance in comparison to DAI. The solubility of DAI-BIP was 73.5-fold higher than the solubility of DAI. The dissolution rate of DAI-BIP quickly reached its equilibrium solubility and it continued to increase till 5.76 µg/mL (1.49 times of the equilibrium solubility). In addition, DAI-BIP showed a 2.03-fold increase for its dissolution performance parameter in comparison to DAI. A parachute effect was observed during the dissolution of DAI-BIP, indicating a function of BIP to maintain the supersaturated state of DAI in solution without the addition of a polymer. It is worth noting that initial computational screening could be problematic and contradictive, depending on the tools used. Therefore, experimental screening is always needed to discover novel cocrystals. To the best of our knowledge, this is the first DAI cocrystal with the structure determined through single crystal XRD measurements which may aid the future discovery of more DAI cocrystals in the future for pharmaceutical applications.

Declaration of interests

None

Acknowledgements

We would like to thank De Montfort University's high-flyer scholarship for Miss Linzie Bolus to conduct the work as part of her PhD project. We also thank Dr. Rachel Armitage for taking the SEM images of crystals.

Reference

1. da Costa JP (2017) A current look at nutraceuticals – Key concepts and future prospects. Trends in Food Science & Technology 62:68-78. doi: https://doi.org/10.1016/j.tifs.2017.02.010

2. Manach C, Scalbert A, Morand C, Rémésy C and Jiménez L (2004) Polyphenols: food sources and bioavailability. The American Journal of Clinical Nutrition 79:727-747. doi: 10.1093/ajcn/79.5.727

3. Manach C, Williamson G, Morand C, Scalbert A and Rémésy C (2005) Bioavailability and bioefficacy of polyphenols in humans. I. Review of 97 bioavailability studies. The American Journal of Clinical Nutrition 81:230S-242S. doi: 10.1093/ajcn/81.1.230S

4. Scalbert A, Manach C, Morand C, Rémésy C and Jiménez L (2005) Dietary Polyphenols and the Prevention of Diseases. Critical Reviews in Food Science and Nutrition 45:287-306. doi: 10.1080/1040869059096

5. Thilakarathna SH and Rupasinghe HPV (2013) Flavonoid bioavailability and attempts for bioavailability enhancement. Nutrients 5:3367-3387. doi: 10.3390/nu5093367

6. Zhao J, Yang J and Xie Y (2019) Improvement strategies for the oral bioavailability of poorly water-soluble flavonoids: An overview. International Journal of Pharmaceutics 570:118642. doi: https://doi.org/10.1016/j.ijpharm.2019.118642

7. Qiao N, Li M, Schlindwein W, Malek N, Davies A and Trappitt G (2011) Pharmaceutical cocrystals: An overview. International Journal of Pharmaceutics 419:1-11. doi: http://dx.doi.org/10.1016/j.ijpharm.2011.07.037

8. Dubey R and Desiraju GR (2015) Combinatorial selection of molecular conformations and supramolecular synthons in quercetin cocrystal landscapes: a route to ternary solids. IUCrJ 2:402-408. doi: doi:10.1107/S2052252515009884

9. Bolla G and Nangia A (2016) Pharmaceutical cocrystals: walking the talk. Chemical Communications 52:8342-8360. doi: 10.1039/C6CC02943D

10. Smith AJ, Kavuru P, Wojtas L, Zaworotko MJ and Shytle RD (2011) Cocrystals of Quercetin with Improved Solubility and Oral Bioavailability. Molecular Pharmaceutics 8:1867-1876. doi: 10.1021/mp200209j

11. Smith AJ, Kavuru P, Arora KK, Kesani S, Tan J, Zaworotko MJ and Shytle RD (2013) Crystal Engineering of Green Tea Epigallocatechin-3-gallate (EGCg) Cocrystals and Pharmacokinetic Modulation in Rats. Molecular Pharmaceutics 10:2948-2961. doi: 10.1021/mp4000794

12. Sinha AS, Maguire AR and Lawrence SE (2015) Cocrystallization of Nutraceuticals. Crystal Growth & Design 15:984-1009. doi: 10.1021/cg501009c

13. Sowa M, Slepokura K and Matczak-Jon E (2013) Cocrystals of fisetin, luteolin and genistein with pyridinecarboxamide coformers: crystal structures, analysis of intermolecular interactions, spectral and thermal characterization. CrystEngComm 15:7696-7708. doi: 10.1039/C3CE41285G

14. He H, Huang Y, Zhang Q, Wang J-R and Mei X (2016) Zwitterionic Cocrystals of Flavonoids and Proline: Solid-State Characterization, Pharmaceutical Properties, and Pharmacokinetic Performance. Crystal Growth & Design 16:2348-2356. doi: 10.1021/acs.cgd.6b00142

15. Kavuru P, Aboarayes D, Arora KK, Clarke HD, Kennedy A, Marshall L, Ong TT, Perman J, Pujari T, Wojtas Ł and Zaworotko MJ (2010) Hierarchy of Supramolecular Synthons: Persistent Hydrogen Bonds Between Carboxylates and Weakly Acidic Hydroxyl Moieties in Cocrystals of Zwitterions. Crystal Growth & Design 10:3568-3584. doi: 10.1021/cg100484a

16. Bis JA, Vishweshwar P, Weyna D and Zaworotko MJ (2007) Hierarchy of Supramolecular Synthons: Persistent Hydroxyl···Pyridine Hydrogen Bonds in Cocrystals That Contain a Cyano Acceptor. Molecular Pharmaceutics 4:401-416. doi: 10.1021/mp070012s

17. Fleischman SG, Kuduva SS, McMahon JA, Moulton B, Bailey Walsh RD, Rodríguez-Hornedo N and Zaworotko MJ (2003) Crystal Engineering of the Composition of Pharmaceutical Phases: Multiple-Component Crystalline Solids Involving Carbamazepine. Crystal Growth & Design 3:909-919. doi: 10.1021/cg034035x

18. Musumeci D, Hunter CA, Prohens R, Scuderi S and McCabe JF (2011) Virtual cocrystal screening. Chemical Science 2:883-890. doi: 10.1039/C0SC00555J

19. Mohammad MA, Alhalaweh A and Velaga SP (2011) Hansen solubility parameter as a tool to predict cocrystal formation. International Journal of Pharmaceutics 407:63-71. doi: http://dx.doi.org/10.1016/j.ijpharm.2011.01.030

20. Abramov YA, Loschen C and Klamt A (2012) Rational Coformer or Solvent Selection for Pharmaceutical Cocrystallization or Desolvation. Journal of Pharmaceutical Sciences 101:3687-3697. doi: 10.1002/jps.23227

21. Issa N, Karamertzanis PG, Welch GWA and Price SL (2009) Can the Formation of Pharmaceutical Cocrystals Be Computationally Predicted? I. Comparison of Lattice Energies. Crystal Growth & Design 9:442-453. doi: 10.1021/cg800685z

22. Ma X-Q, Zhuang C, Wang B-C, Huang Y-F, Chen Q and Lin N (2019) Cocrystal of Apigenin with Higher Solubility, Enhanced Oral Bioavailability, and Anti-inflammatory Effect. Crystal Growth & Design 19:5531-5537. doi: 10.1021/acs.cgd.9b00249

23. Zhang Y-N, Yin H-M, Zhang Y, Zhang D-J, Su X and Kuang H-X (2017) Preparation of a 1:1 cocrystal of genistein with 4,4′-bipyridine. Journal of Crystal Growth 458:103-109. doi: https://doi.org/10.1016/j.jcrysgro.2016.10.084

24. Zhang Y-N, Yin H-M, Zhang Y, Zhang D-J, Su X and Kuang H-X (2017) Cocrystals of kaempferol, quercetin and myricetin with 4,4′-bipyridine: Crystal structures, analyses of intermolecular interactions and antibacterial properties. Journal of Molecular Structure 1130:199-207. doi: https://doi.org/10.1016/j.molstruc.2016.10.034

25. Su X, Zhang Y-n, Yin H-m, Liu L-x, Zhang Y, Wu L-l, Zhang Q, Wang C-x, Zhang L, Zhang Y-j and Zhang Y-x (2019) Preparation of a 1:1.5 cocrystal of kaempferol with 4,4′-bipyridine based on analyzing intermolecular interaction of building units. Journal of Molecular Structure 1177:107-116. doi: https://doi.org/10.1016/j.molstruc.2018.09.050

26. Oswald IDH, Allan DR, McGregor PA, Motherwell WDS, Parsons S and Pulham CR (2002) The formation of paracetamol (acetaminophen) adducts with hydrogen-bond acceptors. Acta Crystallographica Section B 58:1057-1066. doi: 10.1107/S0108768102015987

27. Schultheiss N and Newman A (2009) Pharmaceutical Cocrystals and Their Physicochemical Properties. Crystal Growth & Design 9:2950-2967. doi: 10.1021/cg900129f

28. Jia L, Xu S, Liu S, Du S, Wu S and Gong J (2017) Polymorphs of daidzein and intermolecular interaction effect on solution crystallization. CrystEngComm 19:7146-7153. doi: 10.1039/C7CE01716B

29. Huang G, Xu J and Guo TL (2019) Isoflavone daidzein regulates immune responses in the B6C3F1 and non-obese diabetic (NOD) mice. International Immunopharmacology 71:277-284. doi: https://doi.org/10.1016/j.intimp.2019.03.046

30. Hussain H and Green IR (2017) A patent review of the therapeutic potential of isoflavones (2012-2016). Expert Opinion on Therapeutic Patents 27:1135-1146. doi: 10.1080/13543776.2017.1339791

31. Nan G, Shi J, Huang Y, Sun J, Lv J, Yang G and Li Y (2014) Dissociation Constants and Solubilities of Daidzein and Genistein in Different Solvents. Journal of Chemical & Engineering Data 59:1304-1311. doi: 10.1021/je4010905

32. Qiu F, Chen X-y, Song B, Zhong D-f and Liu C-x (2005) Influence of dosage forms on pharmacokinetics of daidzein and its main metabolite daidzein-7-O-glucuronide in rats. Acta Pharmacologica Sinica 26:1145-1152. doi: 10.1111/j.1745-7254.2005.00187.x

33. Huang S, Xue Q, Xu J, Ruan S and Cai T (2019) Simultaneously Improving the Physicochemical Properties, Dissolution Performance, and Bioavailability of Apigenin and Daidzein by Co-Crystallization With Theophylline. Journal of Pharmaceutical Sciences 108:2982-2993. doi: https://doi.org/10.1016/j.xphs.2019.04.017

34. Bhalla Y, Chadha K, Chadha R and Karan M (2019) Daidzein cocrystals: An opportunity to improve its biopharmaceutical parameters. Heliyon 5. doi: 10.1016/j.heliyon.2019.e02669

35. Guo M, Wang K, Qiao N, Fábián L, Sadiq G and Li M (2017) Insight into Flufenamic Acid Cocrystal Dissolution in the Presence of a Polymer in Solution: from Single Crystal to Powder Dissolution. Molecular Pharmaceutics 14:4583-4596. doi: 10.1021/acs.molpharmaceut.7b00712

36. Sheldrick G (2015) SHELXT - Integrated space-group and crystal-structure determination. Acta Crystallographica Section A 71:3-8. doi: doi:10.1107/S2053273314026370

37. Sheldrick G (2015) Crystal structure refinement with SHELXL. Acta Crystallographica Section C 71:3-8. doi: doi:10.1107/S2053229614024218